

**$\gamma$ - $\alpha$  Isostructural Transition in Cerium**Nicola Lanatà,<sup>1</sup> Yong-Xin Yao,<sup>2,\*</sup> Cai-Zhuang Wang,<sup>2</sup> Kai-Ming Ho,<sup>2</sup>  
Jörg Schmalian,<sup>3</sup> Kristjan Haule,<sup>1</sup> and Gabriel Kotliar<sup>1</sup><sup>1</sup>*Department of Physics and Astronomy, Rutgers University, Piscataway, New Jersey 08856-8019, USA*<sup>2</sup>*Department of Physics and Astronomy and Ames Laboratory—US DOE, Iowa State University, Ames, Iowa 50011, USA*<sup>3</sup>*Karlsruhe Institute of Technology, Institute for Theory of Condensed Matter and Institute for Solid State Research, D-76131 Karlsruhe, Germany*

(Received 13 June 2013; published 5 November 2013)

We present zero-temperature first-principles calculations of elemental cerium and we compute its pressure-volume phase diagram within a theoretical framework able to describe simultaneously both the  $\alpha$  and the  $\gamma$  phases. A surprising result revealed by our study is the presence of a clear signature of the transition at zero temperature and that this signature can be observed if and only if the spin-orbit coupling is taken into account. Our calculations indicate that the transition line in the pressure-temperature phase diagram of this material has a low- $T$  critical point at negative pressures, placed very close to zero temperature. This suggests that cerium is very close to being “quantum critical,” in agreement with recent experiments.

DOI: [10.1103/PhysRevLett.111.196801](https://doi.org/10.1103/PhysRevLett.111.196801)

PACS numbers: 71.15.-m, 71.20.Be, 71.27.+a, 73.63.Kv

Below the critical temperature  $T_c \simeq 600$  K, an isostructural transition, named the  $\gamma$ - $\alpha$  transition, can be induced in cerium by applying pressure [1]. This transition is first order and is accompanied by a sizable volume collapse. The  $\gamma$ - $\alpha$  transition was discovered in 1949 [2]. Since then, a lot of theoretical and experimental work has been devoted to its understanding. The great interest in this phenomenon arises from the fact that the transition is isostructural; i.e., the lattice structure of the system is equal in the two phases. Furthermore, the possibility that the underlying mechanism lies in the electronic structure only—i.e., without it being necessary to involve other effects—makes cerium a potential theoretical testing ground for basic concepts of correlated electron systems. Two main theoretical pictures are still under debate to explain the volume collapse: the Kondo volume collapse (KVC) [3,4] and the orbital-selective Mott transition within the Hubbard model (HM) [5]. According to the KVC, the transition is induced by the rapid change of the coherence temperature across the transition boundaries, which affect dramatically the structure of the conduction  $spd$  electrons through the Kondo effect. According to the HM, instead, it is the hopping between  $f$  orbitals that changes drastically across the transition between the  $\alpha$  phase (with delocalized  $f$  electrons) and the  $\gamma$  phase (with localized  $f$  electrons), as for the Mott transition in the Hubbard model.

Consistently with both the HM and the KVC pictures, the  $f$  electrons are strongly correlated both in the  $\alpha$  and in the  $\gamma$  phases. This fact is clearly indicated, e.g., by the photoemission spectra, which are known experimentally [6–8] and theoretically [9–11]. Despite this similarity, there is a key difference between these two models: while the KVC attributes a very important role to the interplay

between the localized  $4f$  orbitals and the itinerant  $spd$  conduction bands, the itinerant electrons are “spectators” in the HM picture.

The development of local density approximation plus dynamical mean field theory (LDA + DMFT) [12] results [13–15] has successfully reproduced many aspects of this transition, and different aspects of these studies can be understood in both physical pictures. There are still fundamental questions which have not been answered. (1) What is the role of the spin-orbit interaction (SOC) for the volume collapse? (2) What is the fate of the pressure-temperature transition line at very low temperatures [16–18]? (3) Can a first-principles-based theory be made computationally efficient so as to access both the  $\gamma$  and the  $\alpha$  cerium at zero temperature?

Because of the complexity of the problem, it is clear that, in order to be conclusive, a theoretical explanation of the  $\gamma$ - $\alpha$  transition needs to be supported by first-principles calculations which not only are able to take into account both the details of the band structure and the strong-correlation effects but are also able to evaluate precisely the pressure-volume phase diagram. For this purpose, it is crucial that the computation of the total energy is essentially free of numerical error. Another key requirement is that the two phases are treated within the same theoretical framework. In this work, we use a combination of density functional theory and the Gutzwiller approximation (LDA + GA) [19–23], which satisfies all of these requirements. Recently, we have established formally [24] that this method can be viewed as an instance of LDA + DMFT, using slave bosons (or the Gutzwiller method) as the DMFT impurity solver [14]. This insight enabled a new efficient charge self-consistent implementation of the LDA + GA method on top [25] of the Linearized

Augmented Plane Wave Density Functional Theory code WIEN2K [26], which removes many of the approximations inherent in previous studies. As a benchmark, in the Supplemental Material [27], we also present LDA + DMFT calculations for cerium. The very good agreement between the two methods gives us further confirmation that the results presented in this work are indeed reliable.

We employ the general Slater-Condon parametrization of the on-site interaction, assuming a Hund's coupling constant  $J = 0.7$  eV [28]. Since the value  $U$  of the interaction strength is generally difficult to establish accurately (due to its strong sensitivity to the screening effect), in this work, we perform calculations scanning different values of  $U$ . Our calculations are all performed at zero temperature.

In the upper panels of Fig. 1, we illustrate our theoretical energy-volume diagrams for different values of  $U$ . The results are shown both by taking into account the SOC (left panels) and by neglecting it in the calculation (right panels). The corresponding pressure-volume curves, obtained from  $P = -dE/dV$ , are shown in the lower panels, in comparison with the experimental data at room temperature of Refs. [29,30]. The agreement with the

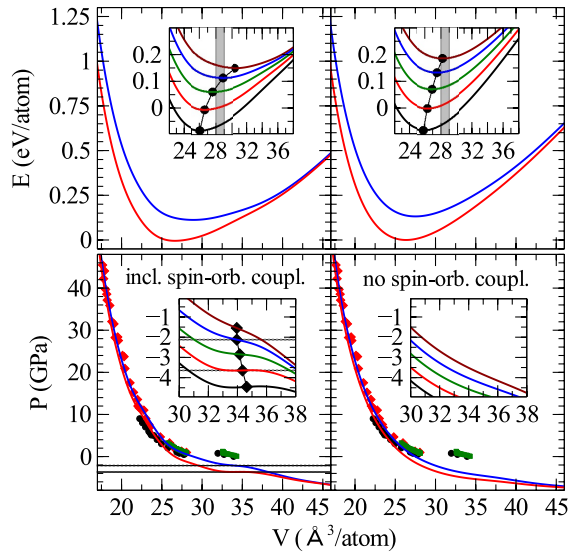


FIG. 1 (color online). Total energy as a function of the volume (upper panels) and corresponding theoretical pressure-volume curves for  $U = 5, 6$  eV,  $J = 0.7$  eV, in comparison with the experimental data (lower panels). The experimental data relate to measurements at room temperature (black circles from Ref. [29], red diamonds from Ref. [30], and green squares from Ref. [35]), while our theoretical calculations are all obtained at zero temperature. The curves in the insets are obtained for all  $U$ 's from 4.5 to 6.5 eV (from lower to higher total energies) with steps of 0.5 eV. Our results are shown both with (left panels) and without (right panels) taking into account the spin-orbit coupling. The vertical shaded lines in the upper insets indicate the experimental volume at ambient pressure. The horizontal dotted lines in the lower-left panel and the black diamonds in its inset indicate the pressures where the bulk modulus  $\mathcal{K} = -VdP/dV$  is minimum.

experiment is good, especially for  $U = 6$  eV, which is the value that reproduces the experimental equilibrium volume  $V_{\text{eq}} \approx 28.5 \text{ \AA}^3/\text{atom}$  [29–31] (see the inset of the upper-left panel). The small discrepancies at larger  $V$  are likely, at least in part, due to the entropy, as our calculations were performed at zero temperature. Note that  $U = 6$  eV was also previously computed within the constrained LDA method [9,32], which gives us further confidence that this is the optimal value of the correlation strength for cerium.

Remarkably, we observe a change of sign in the bulk modulus  $\mathcal{K} = -VdP/dV < 0$ —which is the signal of a first-order isostructural transition—for any  $U \leq U_c \approx 5.5$  eV (see the pressure-volume curves in the lower-panel insets of Fig. 1), while at  $U = U_c$ , the transition becomes second order, with a  $\mathcal{K} = 0$  minimum bulk modulus. A signature of the transition, i.e., a local minimum of the bulk modulus, is still present for any interaction strength; see the black diamonds in the inset of the lower-left panel of Fig. 1. We point out that this feature of the pressure-volume curve is observed *only* if the SOC is taken into account—which is a clear indication of its key role in the physics underlying the  $\gamma$ - $\alpha$  transition. Note also that for  $U = 6$  eV, the crossover point occurs at  $P \approx -2$  GPa, which is close to the expected zero-temperature value  $P_{\text{exp}} \approx -1$  GPa extrapolated from the experimental data of Ref. [1].

In order to better understand the role of the SOC, we consider the local  $f$  entanglement entropy

$$S_f[\rho_f] = -\text{Tr}[\rho_f \ln \rho_f], \quad (1)$$

where  $\rho_f$  is the reduced density matrix of the system in the  $f$  local subspace. The value of  $S_f$  is a measure of how much the  $f$  electrons are entangled with the rest of the environment. In Fig. 2, the behavior of  $S_f$  is shown as a function of the volume for two values of  $U$ . Remarkably, if (and only if) the SOC is taken into account, a clear crossover is visible in the correspondence of the signature of the volume collapse, i.e., in the correspondence of the minimum of the bulk modulus  $\mathcal{K}$ , which is indicated by black diamonds in the inset of the lower-left panel of Fig. 1.

In the  $\alpha$  phase, as expected,  $S_f$  is not sensitive to the spin-orbit splitting, indicating that the local fluctuations induced in the  $f$  local space by the coupling with its environment are very large. By increasing the volume, the fluctuations between the  $J = 5/2$   $f^1$  subspace and the other local configurations are increasingly suppressed. The crossover point identifies the situation in which the above-mentioned fluctuations are sufficiently small to be hampered by the spin-orbit splitting. This is clearly demonstrated by the fact that in the  $\gamma$  phase, when the SOC is taken into account,  $S_f \approx \ln 6$ —where  $6 = 2 \times 5/2 + 1$  is the degeneracy of the  $5/2$  eigenspace at  $n_f = 1$ . We point out that the above-mentioned local fluctuations are generated only by the entanglement and so are present even if the actual temperature of the system is zero—as in our

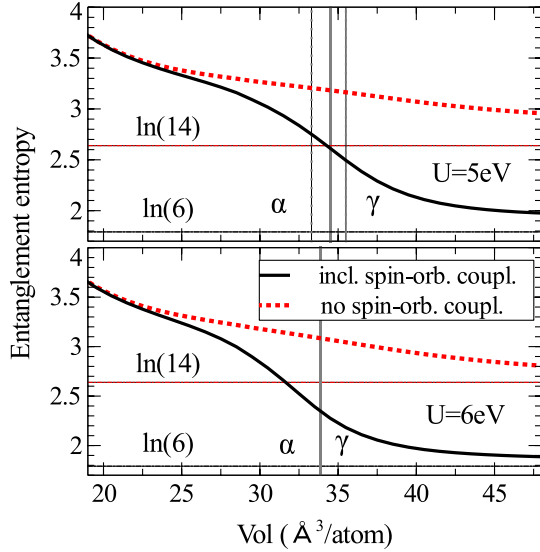


FIG. 2 (color online). Local entanglement entropy of the  $f$  electrons as a function of the volume per atom of the system for  $U = 5$  eV (upper panel) and  $U = 6$  eV (lower panel) at fixed  $J = 0.7$  eV. The entanglement entropy is reported both for the case with (lines) and without (dots) the SOC. The horizontal lines correspond to 14, which is the dimension of the single-particle local space of the  $f$  electrons, and to  $6 = 2 \times 5/2 + 1$ , which is the degeneracy of the  $5/2$   $f$  electrons within the single-particle local space. The vertical solid lines indicate the signature of the transition in the pressure-volume diagram, and the dotted vertical lines indicate the boundary of the  $\gamma$ - $\alpha$  transition (which occurs only for  $U \leq U_c \simeq 5.5$  eV) according to the equal-area construction [36].

calculations. As we are going to show, the main source of entanglement is the hybridization between the  $f$  and the  $spd$  electrons.

A further insight of the problem can be achieved by inspecting the ground-state expectation values of the non-local energy components of the effective Hamiltonian  $\hat{\mathcal{H}}$  whose ground state provides our theoretical solution [12,21]. The nonlocal part  $\hat{T}$  of  $\hat{\mathcal{H}}$  can be concisely represented as

$$\hat{T} = \hat{T}_{ff} + \hat{T}_{fc} + \hat{T}_{cc}, \quad (2)$$

where the symbol  $c$  represents all of the  $spd$  conduction electrons, and  $\hat{T}_{ff}$ ,  $\hat{T}_{fc}$ , and  $\hat{T}_{cc}$  represent the nonlocal “hopping” terms between  $f$ - $f$ ,  $f$ - $c$ , and  $c$ - $c$  electrons, respectively. In Fig. 3, the ground-state expectation values of the  $f$ - $c$  and the  $f$ - $f$  components of  $\hat{T}$  are shown for two values of  $U$ . These energies represent the Kondo and the Hubbard energy scales of the problem, respectively. In agreement with the KVC model of the transition, we observe that the Kondo energy scale is about 1 order of magnitude bigger than the Hubbard energy scale, which is already very small before the crossover point, as expected [33]. This confirms that the main source of entanglement

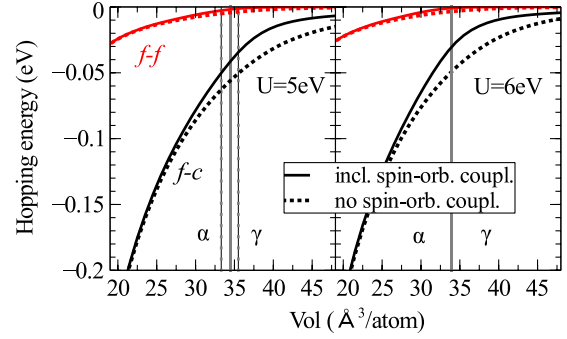


FIG. 3 (color online). Ground-state expectation values of the  $f$ - $c$  and the  $f$ - $f$  effective hopping energies as a function of the volume per atom of the system. The energies are reported for  $U = 5$  eV (left panel) and  $U = 6$  eV (right panel) at fixed  $J = 0.7$  eV, both for the case with (lines) and without (dots) the spin-orbit coupling. The vertical solid lines indicate the signature of the transition in the pressure-volume diagram, and the dotted vertical lines indicate the boundary of the  $\gamma$ - $\alpha$  transition (which occurs only for  $U \leq U_c \simeq 5.5$  eV) according to the equal-area construction [36].

between the  $f$  local space and its environment is the hybridization between the  $f$  and the  $spd$  electrons. Note that when the SOC is taken into account, a more rapid suppression of the Kondo energy scale is observed concomitantly with the crossover region.

We have already observed that even though the behavior of the entanglement entropy (and of the Kondo energy scale) is qualitatively the same for all  $U$ 's, no transition can be found for  $U \geq U_c \simeq 5.5$  eV at zero temperature; see Figs. 1 and 2. The reason is the following. The local crossover, which induces a reduction of the bulk modulus of the system, occurs at lower volumes for larger  $U$ ; see the black diamonds in the inset of the lower-left panel of Fig. 1. On the other hand, the bulk modulus becomes larger at smaller volumes (even when the SOC is not taken into account); see the pressure-volume curves in the lower panels of Fig. 1. For this reason, if  $U$  is large enough, it becomes impossible for the SOC to make the bulk modulus negative, i.e., to induce the volume collapse. It follows that, in principle, there are two possible scenarios: (i) the  $\gamma$ - $\alpha$  transition also exists at zero temperature, or (ii) the transition line ends at a certain finite critical temperature (at negative pressures). As we mentioned before,  $U \simeq 6$  eV—which is indeed very close to  $U_c$ —is a physically reasonable value for cerium. This suggests that cerium is placed essentially in the middle between the two above-mentioned scenarios, i.e., that the  $\gamma$ - $\alpha$  transition line ends very close to zero temperature. Note that this finding is in qualitative agreement with the experimental results of Ref. [34].

It is useful to examine how the local crossover induced by the SOC reflects on the quasiparticle renormalization weights and the on-site configuration probabilities. In the first panel of Fig. 4 are illustrated the averaged quasiparticle renormalization weights  $Z$  of the  $7/2$  and  $5/2$   $f$

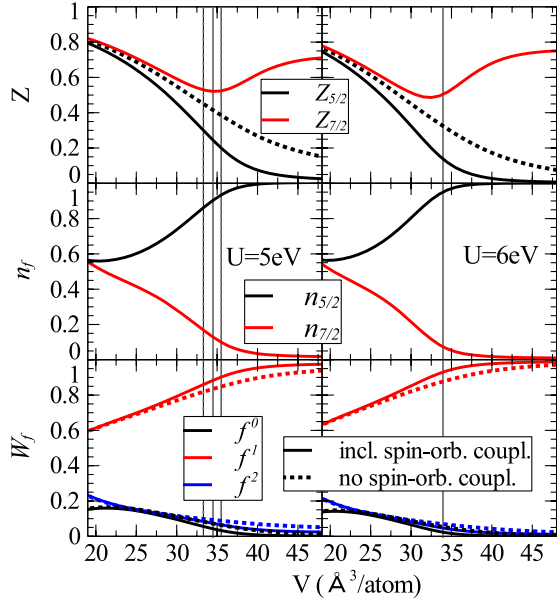


FIG. 4 (color online). Quasiparticle renormalization weights of the 7/2 and 5/2  $f$  electrons (upper panels), 7/2 and 5/2  $f$  orbital populations (central panels), and  $f$  configuration probabilities (lower panels), as a function of the volume of the system. The renormalization weights and the configuration probabilities are reported both for the cases with and without the spin-orbit coupling, for  $U=5\text{eV}$  (left panels) and  $U=6\text{eV}$  (right panels) at fixed  $J=0.7\text{eV}$ . The vertical solid lines indicate the signature of the transition in the pressure-volume diagram, and the dotted vertical lines indicate the boundary of the  $\gamma$ - $\alpha$  transition (which occurs only for  $U \leq U_c \approx 5.5\text{eV}$ ) according to the equal-area construction [36].

electrons—which are significantly different because of the spin-orbit effect. As expected [33], the  $f$  electrons are correlated ( $Z$  is significantly smaller than 1) even in the  $\alpha$  phase, and the two  $Z$ 's monotonically decrease by increasing the volume at higher pressures. Nevertheless, they develop a qualitatively different behavior at the crossover point. While the 5/2 electrons undergo a clear crossover toward a localized phase “disentangled” by the conduction electrons, the 7/2 electrons remain screened, but they rapidly disappear afterwards, so that they are essentially absent in the  $\gamma$  phase; see the second panel of Fig. 4. As shown by the  $f$  configuration probabilities in the third panel of Fig. 4, the SOC speeds up the formation of the  $4f^1$  local moment. In other words, the SOC acts as a “catalyst,” which favors the disentanglement between the  $4f$  electrons and the conduction electrons.

In conclusion, we have performed first-principles calculations on cerium using a new efficient implementation of the LDA + GA method. For the physical value of  $U$  in cerium  $U \approx 6\text{eV}$  [9,32], a sharp crossover is observed in many physical quantities around the volume where the bulk modulus is minimum. This finding is robust against changes in  $U$ , but the details are different. For  $U < U_c$ , at  $T = 0$ , there is a first-order transition at a given negative

value of the pressure, while for  $U > U_c$ , this transition becomes a sharp crossover. At  $U_c$ , there is a second-order quantum critical point in the phase diagram. Our estimate for the critical interaction strength  $U_c \approx 5.5\text{eV}$  is very close to the physical value of the interaction strength in cerium. This finding suggests that elemental cerium is a critical element, consistently with the experiments [34]. Our results demonstrate the importance of the SOC for the volume collapse in cerium, which is neatly captured by the rapid variation of the entanglement entropy of the  $f$  electrons in the region around the minimum of the bulk modulus. In the  $\alpha$  phase, at small  $V$ , the  $f$  levels are strongly hybridized with the conduction electrons, and the quasiparticle weights and the pressure are only weakly dependent on the spin-orbit interaction. In this regime, the system effectively behaves as if the  $f$ -level degeneracy was of the order of magnitude of 14. In the  $\gamma$  phase, at large  $V$ , the spin-orbit splitting becomes more important and substantially reduces the effective  $f$ -level degeneracy. The fact that the quasiparticle weight in the  $\gamma$  phase is much smaller when the SOC is taken into account (see Fig. 4) can be interpreted as a consequence of the above-mentioned reduction of effective  $f$ -level degeneracy—a well-known effect in the theory of the single-ion Kondo impurity. As in the early Kondo volume-collapse theory [3],  $\partial Z/\partial V$  contributes to the pressure. However, some qualitative features of our solution, such as the form of the pressure-volume phase diagram, show that other physical elements, such as the changes in the charge density induced by the correlations, also have to be included in realistic theories of this material. The physical mechanism underlying the  $\gamma$ - $\alpha$  transition in cerium is a possible paradigm for the volume-collapse transitions in  $4f$  and  $5f$  systems, which is a major challenge in condensed matter physics.

N.L. and Y.-X.Y. thank XiaoYu Deng and Robert McQueeney for useful discussions. The collaboration was supported by the U.S. Department of Energy through the Computational Materials and Chemical Sciences Network CMSCN. Research at Ames Laboratory was supported by the U.S. Department of Energy, Office of Basic Energy Sciences, Division of Materials Sciences and Engineering. Ames Laboratory is operated for the U.S. Department of Energy by Iowa State University under Contract No. DE-AC02-07CH11358.

\*Corresponding author.  
ykent@iastate.edu

- [1] D. C. Koskenmaki and K. A. G., Jr., in *Metals*, edited by J. Karl, A. Gschneidner, and L. Eyring, Handbook on the Physics and Chemistry of Rare Earths Vol. 1 (Elsevier, New York, 1978), p. 337.
- [2] A. W. Lawson and T.-Y. Tang, *Phys. Rev.* **76**, 301 (1949).
- [3] J. W. Allen and R. M. Martin, *Phys. Rev. Lett.* **49**, 1106 (1982).

- [4] M. Lavagna, C. Lacroix, and M. Cyrot, *Phys. Lett.* **90A**, 210 (1982).
- [5] B. Johansson, *Philos. Mag.* **30**, 469 (1974).
- [6] D.M. Wieliczka, C.G. Olson, and D.W. Lynch, *Phys. Rev. Lett.* **52**, 2180 (1984).
- [7] E. Weschke, C. Laubschat, T. Simmons, M. Domke, O. Strebel, and G. Kaindl, *Phys. Rev. B* **44**, 8304 (1991).
- [8] F. Patthey, B. Delley, W.D. Schneider, and Y. Baer, *Phys. Rev. Lett.* **55**, 1518 (1985).
- [9] M.B. Zöflf, I.A. Nekrasov, T. Pruschke, V.I. Anisimov, and J. Keller, *Phys. Rev. Lett.* **87**, 276403 (2001).
- [10] K. Held, A.K. McMahan, and R.T. Scalettar, *Phys. Rev. Lett.* **87**, 276404 (2001).
- [11] A.K. McMahan, K. Held, and R.T. Scalettar, *Phys. Rev. B* **67**, 075108 (2003).
- [12] G. Kotliar, S.Y. Savrasov, K. Haule, V.S. Oudovenko, O. Parcollet, and C.A. Marianetti, *Rev. Mod. Phys.* **78**, 865 (2006).
- [13] K. Haule, V. Oudovenko, S.Y. Savrasov, and G. Kotliar, *Phys. Rev. Lett.* **94**, 036401 (2005).
- [14] G. Kotliar, S.Y. Savrasov, K. Haule, V.S. Oudovenko, O. Parcollet, and C.A. Marianetti, *Rev. Mod. Phys.* **78**, 865 (2006).
- [15] K.T. Moore and G. van der Laan, *Rev. Mod. Phys.* **81**, 235 (2009).
- [16] L. de' Medici, A. Georges, G. Kotliar, and S. Biermann, *Phys. Rev. Lett.* **95**, 066402 (2005).
- [17] B. Amadon, S. Biermann, A. Georges, and F. Aryasetiawan, *Phys. Rev. Lett.* **96**, 066402 (2006).
- [18] M. Casadei, X. Ren, P. Rinke, A. Rubio, and M. Scheffler, *Phys. Rev. Lett.* **109**, 146402 (2012).
- [19] M.C. Gutzwiller, *Phys. Rev.* **137**, A1726 (1965).
- [20] N.E. Zein, *Phys. Rev. B* **52**, 11 813 (1995).
- [21] X.Y. Deng, L. Wang, X. Dai, and Z. Fang, *Phys. Rev. B* **79**, 075114 (2009).
- [22] K.M. Ho, J. Schmalian, and C.Z. Wang, *Phys. Rev. B* **77**, 073101 (2008).
- [23] N. Lanatà, H.U.R. Strand, X. Dai, and B. Hellsing, *Phys. Rev. B* **85**, 035133 (2012).
- [24] N. Lanatà, Y.X. Yao, and G. Kotliar (unpublished).
- [25] Y.X. Yao, N. Lanatà, and G. Kotliar (unpublished).
- [26] P. Blaha, K. Schwarz, G. Madsen, D. Kvasnicka, and J. Luitz, computer code WIEN2K, University of Technology, Vienna, 2001.
- [27] See Supplemental Material <http://link.aps.org/supplemental/10.1103/PhysRevLett.111.196801> for technical remarks, benchmark calculations with LDA + DMFT and note on the importance of the charge self-consistency.
- [28] R.D. Cowan, *The Theory of Atomic Structure and Spectra* (University of California Press, Berkeley, 1981).
- [29] W.H. Zachariasen and F.H. Ellinger, *Acta Crystallogr. Sect. A* **33**, 155 (1977).
- [30] J. Olsen, L. Gerward, U. Benedict, and J.-P. Itié, *Physica (Amsterdam)* **133B+C**, 129 (1985).
- [31] F.H. Ellinger and W.H. Zachariasen, *Phys. Rev. Lett.* **32**, 773 (1974).
- [32] A. McMahan, C. Huscroft, R. Scalettar, and E. Pollock, *J. Comput.-Aided Mater. Des.* **5**, 131 (1998).
- [33] A.P. Murani, S.J. Levett, and J.W. Taylor, *Phys. Rev. Lett.* **95**, 256403 (2005).
- [34] J.C. Lashley, A.C. Lawson, J.C. Cooley, B. Mihaila, C.P. Opeil, L. Pham, W.L. Hults, J.L. Smith, G.M. Schmiedeshoff, F.R. Drymiotis *et al.*, *Phys. Rev. Lett.* **97**, 235701 (2006).
- [35] M.J. Lipp, A.P. Sorini, J. Bradley, B. Maddox, K.T. Moore, H. Cynn, T.P. Devereaux, Y. Xiao, P. Chow, and W.J. Evans, *Phys. Rev. Lett.* **109**, 195705 (2012).
- [36] L.D. Landau and E.M. Lifshitz, *Statistical Physics* (Pergamon, London, 1958).